Improving Antibiotic Properties using a Crystal Engineering Approach

Merve Arpacıoğlu[1,*], Mariama Djaló[1], Teresa Neuparth[1], Andreia Cunha[1], Vânia André[1], M. Teresa Duarte[1]

[1] Centro de Química Estrutural, Instituto Superior Técnico, Univiersidade de Lisboa, Av. Rovisco Pais, Lisboa, Portugal

** E-mail: mervearpacioglu@gmail.com*

Abstract

This study aims to expand the pharmaceutical solid-state forms of Sparfloxacin (SPX) by using crystal engineering principles. This drug is an antibiotic and it offers a trade-off between high solubility and low membrane permeability due to its zwitterionic nature. Therefore, the ultimate goal is to develop new multicomponent crystal forms of SPX with different physicochemical properties. After a polymorphic screening, the multicomponent forms of SPX are extended within this study by the use of 4-Aminosalicylic acid (4-ASA), 3-Aminobenzoic acid (3-ABA), Anthranilic acid (AA), and Nalidixic acid (NA) as co-formers. The solubility of the new multicomponent forms was improved compared with SPX owing to the salt nature of the multicomponent forms obtained. Lastly, it is shown that all the new multicomponent forms are stable under 78% room humidity.

Keywords: Crystal engineering, supramolecular synthons, pharmaceutical crystal forms, Sparfloxacin

Introduction

In today's world, it is remarkably important to investigate all solid forms of drugs in order to overcome the issues of active pharmaceutical ingredients (APIs) with the hope of obtaining desired physicochemical properties.[1-4] Polymorphs, solvates, hydrates, and multicomponent forms including co-crystals and salts, are the pharmaceutical solid-state forms of APIs and the interest in these crystalline phases of APIs has increased in the last two decades[5-10] since these crystalline forms have proved advantageous in tailoring APIs physicochemical properties, such as solubility, bioavailability, permeability, stability, tabletability melting point.[11-13] Crystal engineering has taken the lead in the rational design, synthesis, and characterization of all these forms.[14]

SPX is a broad-spectrum antimicrobial agent from the class of fluoroquinolone antibiotic[15] which was launched as a medicine in 1935 for the treatment of *streptococci* and community-acquired lower respiratory tract infection under the name of Zagam. As the other quinolones, the antimicrobial activity of SPX stems from inhibition of topoisomerase II (DNA gyrase) and topoisomerase I, which are enzymes contributing to bacterial DNA transcription, and replication.[16-17] It possesses in vitro activity against both gram-negative and gram-positive microorganisms.[18] Compared with its counterparts, SPX displays enhanced microbial activity against a wide range of gram-positive pathogens and better in-vitro activity against gram-positive *cocci* and anaerobe microorganisms.[19-20] Whilst most of adverse side effects are similar to other fluoroquinolones, SPX has a higher potential in phototoxicity,[21-22] for that reason, in 2001, the medicine was withdrawn from the market.[23]

From chemistry point of view, SPX *(Figure 1 (a))* naturally offers a trade-off between high solubility and membrane permeability due to being a zwitterionic drug.[24] Hence, stabilizing the solid to enhance its bioavailability is highly important. In Cambridge Structural Database (CSD)[25], there are three different forms reported including one anhydrous form, and two different hydrates.[19, 26] Additionally it is possible to find studies of multicomponent forms of SPX published in CSD[25] database, e.g. salt of SPX with tetrafluoroborate,[27] and ionic metal complexes with zinc,[28] and copper.[27] Gunnam et al. showed the possible co-crystal formation between SPX and methyl, ethyl, isobutyl paraben via amino phenol synthon recognition.[24] To the best of our knowledge, there are no other studies reporting multicomponent forms of SPX.

Herein, we report acetonitrile (ACN) solvate as well as five different new crystalline salts of SPX with the use of carboxylic acid derivatives: 4-ASA, 3-ABA, AA *(Figure 1(b))* inspired by the previous works in

which relative strength of piperazine ring of floxacin derivative drugs as a base towards carboxylic acid has been reported.[29-30] The solubility of the new multicomponent forms was improved compared with SPX, owing to salt nature of the new forms. Furthermore, it is noteworthy to mention that 4-ASA is an antibiotic which is used in therapy of tuberculosis. The combination of SPX and 4-ASA molecules within one crystal lattice offers a novel therapy opportunity for the treatment of tuberculosis, which can possibly exhibit a superior antimicrobial activity.[31-32]

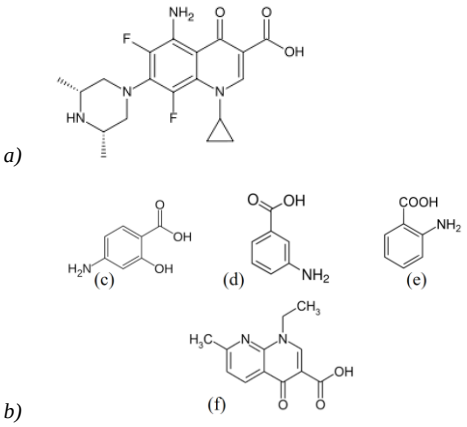

Figure 1 The molecular structures of a) Sparfloxacin (SPX) b) GRAS co-formers 4-ASA (c), 3-ABA (d), AA (e), NA (f) respectively

Results and Discussion

Throughout this study, polymorphic, co-crystals and salts screening of Sparfloxacin were performed. The results are mentioned below.

Polymorphic screening of SPX

Polymorphic screening of Sparfloxacin was done recurring to different solvents. All the experimental trials were characterized by powder X-ray diffraction (PXRD) and the results are demonstrated in *Figure 2*.

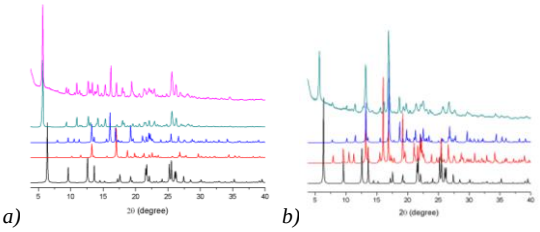

Figure 2 The PXRD results of polymorphic screening of SPX with a) DMSO-slurry rxn (green) and solution chemistry (pink line) b) EtOH-slurry rxn (green line). Black, red and blue lines correspond to SPX forms deposited in the CSD with JEKMOB, COQWOU, COQWU01 refcodes respectively.

According to the results, it can be mentioned that two different new forms are obtained with the use of DMSO, and EtOH as a solvents *(Figure 2*). However, it remains unknown if these forms are polymorphs or solvates of SPX since it was not possible to determine their crystal structures.

Surprisingly, ACN solvate of SPX was encountered throughout the co-crystal investigation of SPX with nalidixic acid (NA). This ACN solvate was only obtained in the presence of nalidixic acid, precluding the achievement of a pure phase. The mentioned PXRD results are shown in *Figure 3*.

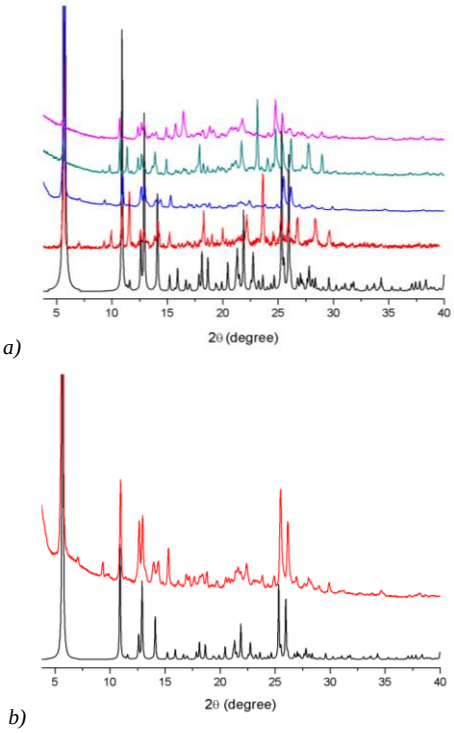

Figure 3 The PXRD results of ACN solvate experimental procedures a) with (red and green line) and without (blue and pink line) the use of NA b) with 4:1 SPX:NA mol ratio.

The formation of the ACN solvate was confirmed by SCXRD results (*Figure 4*).

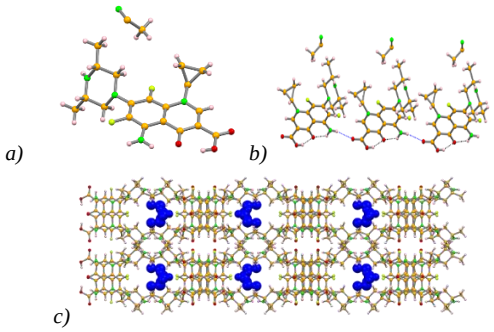

Figure 4 Illustration of ACN solvate crystal structure depicting: (a) the asymmetric unit; (b) the intermolecular (black) and

intermolecular (blue) hydrogen bonds established; and (c) the supramolecular arrangement in a view along the c axis

The asymmetric unit of the ACN's solvate consists of one molecule of SPX and an acetonitrile molecule, with the ACN molecule residing on a special position, with half occupation factors. Both sparfloxacin intramolecular hydrogen bonds established between the N-H_{NH2} and the carbonyl, and the O-H_{COOH} and the carbonyl are maintained in the new solvate. In addition, the type of interactions between consecutive SPX molecules (N-H_{NH2} ⋯ O-H_{COOH}) is similar to the interactions observed in SPX alone (*Figure 4* (b)).

Additionally, TGA-DSC measurement was also carried out in order to further confirm the presence of ACN molecules (*Figure ES1*). According to the result, it is possible to relate the weight loss approximately 2.58 % at 136ºC. This weight loss is in in the agreement with theoretical calculation. However, the bulk sample was not a pure phase, therefore, definite conclusions cannot be withdrawn in these conditions.

Screening of Co-crystals and Salts of Sparfloxacin

With the application of 4-ASA, 3ABA and AA, six different salts were obtained in this study. The names of these salts are mentioned as **SPX:4ASA Form I**, **SPX:4ASA Form II**, **SPX:4ASA Form III**, **SPX:3ABA Form I**, **SPX:3ABA Form II** and **SPX-AA**.

Structural characterization of SPX:4ASA salts

According to SCXRD data, the asymmetric unit of **SPX:4ASA Form I** corresponds to one cationic SPX and one anionic 4ASA and a cluster with multiple disordered water molecules. The accurate number of water molecules was not possible to confirm by SCXRD. The typical intramolecular bonds in SPX established between the N-H_{NH2} and the carbonyl and the O-H_{COOH} and the carbonyl, as well as the intramolecular O-H_{COOH} ⋯ O_{OH} hydrogen bond of 4-ASA are maintained. However, the N-H_{NH2} ⋯ O-H_{COOH} interaction between SPX is disrupted to give rise to interactions with 4-ASA via N-$H_{NH2,SPX}$⋯ $O_{OH,4ASA}$ hydrogen bonds (*Figure 5)*.

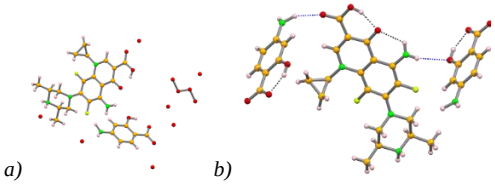

a) *b)*

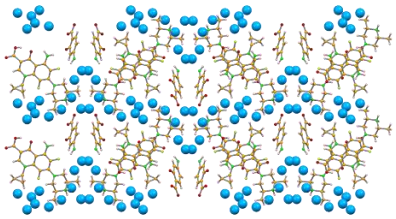

c)

Figure 5 Illustration of SPX:4ASA Form I crystal structure depicting:: (a) the asymmetric unit with the disordered water cluster; (b) the intramolecular (black) and intermolecular (blue) hydrogen bonds established between SPX and 4ASA; and (c) the crystal packing

The asymmetric unit of **SPX:4ASA Form II** consists of one cationic SPX an one anionic 4ASA. The intramolecular interactions of both SPX and 4-ASA mentioned above are still maintained**.** However, in this anhydrous form the interaction between 4ASA and SPX is established via the cationic NH_2^+ moiety of SPX. In a view along the *b* axis, the supramolecular arrangement shows a honey comb like packing (*Figure 6*). However, this form was not obtained as a pure phase (Figure ES7).

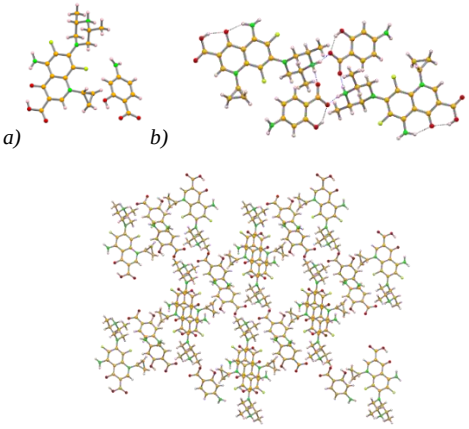

a) *b)* *c)*

Figure 6 Illustration of Form II crystal structure depicting: (a) the asymmetric unit; (b) the intramolecular (black) and intermolecular (blue) interactions; and (c) the supramolecular arrangement in a view along the b axis

Since there is no good data refinement with **SPX:4ASA Form III**, SCXRD result is not shown here. However, the formation of a new form was confirmed with PXRD measurement (*Figure ES6)*.

Structural characterization of SPX-3ABA salts

Based on the SCXRD result of **SPX:3ABA Form I**, the asymmetric unit involves one cationic SPX, one anionic 3-ABA and two water molecules. The

typical intramolecular bonds in SPX are again maintained, as well as the N-H_{NH2} ⋯ O-H_{COOH} interactions between SPX giving rise to zigzag chains. The interaction with 3ABA is established via the cationic NH_2^+ moiety (N-$H_{NH2+,SPX}$ ⋯ $O_{COO-,3ABA}$) and the water molecules (N-$H_{NH2+,SPX}$ ⋯ O-H_{H2O} ⋯ $O_{COO-,3ABA}$), giving rise to a supramolecular arrangement in which zig-zag chains of SPX are alternated by a double layer of 3ABA and water molecules (*Figure 7*).

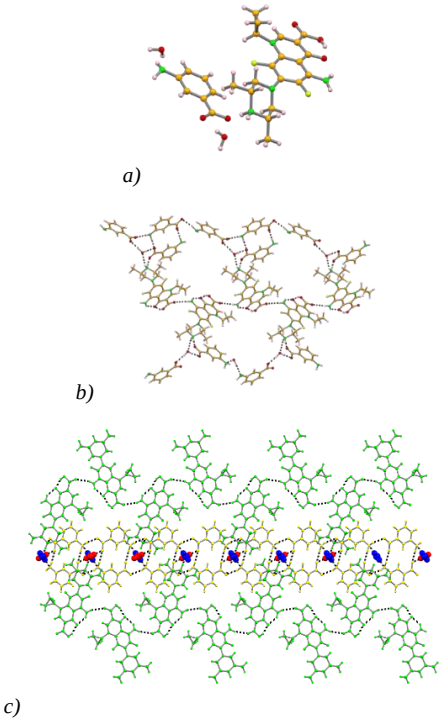

Figure 7 The illustration of SPX:3ABA Form I crystal structure depicting a) the asymmetric unit; b) the hydrogen bonding between SPX, 3ABA and water molecules; c) the crystal packing showing the zig-zag chains of SPX (green) intercalated with chains of 3ABA (yellow) and water molecules (red and blue, using spacefill representation)

The asymmetric unit of **SPX:3ABA Form II** involves one cationic SPX, one anionic 3-ABA and a disordered water cluster residing over a special position. The typical intramolecular bonds in SPX are again maintained, but the N-H_{NH2} ⋯ O-H_{COOH} interaction is disrupted to give rise to the interaction with 3-ABA(N-$H_{NH2,SPX}$⋯$N_{NH2,3-ABA}$ and N-$H_{NH2,3ABA}$⋯$O_{COOH,SPX}$). In the overall supramolecular packing, it is possible to see ladder-like chains of 3-ABA, separate rows of SPX, and water clusters (*Figure 8*).

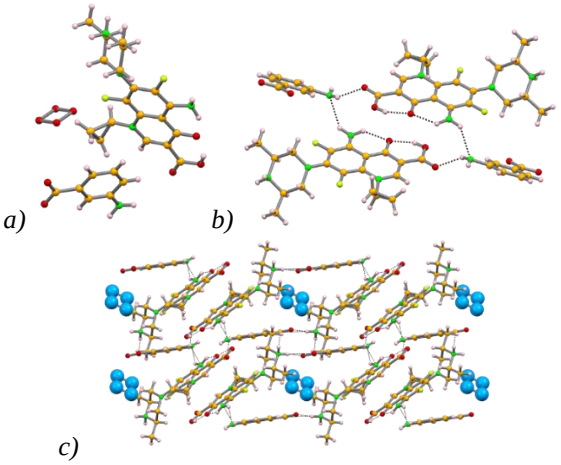

Figure 8 The illustration of SPX:3ABA Form II crystal structure depicting (a) the asymmetric unit; (b) the hydrogen bonding between SPX and 3ABA; (c) the crystal packing showing the ladder-like chains of 3ABA separate rows of SPX and water clusters (blue)

Structural characterization of SPX:AA salt

According to SCXRD result of **SPX:AA** The asymmetric unit of SPX and AA salt contains one cationic SPX and one anionic AA. The typical intramolecular bonds in SPX are maintained, as well as the zigzag chains formed by the N-H_{NH2} ⋯ O-H_{COOH} interactions between SPX. The interaction with AA is established via the cationic moiety of SPX (N-$H_{NH2+,SPX}$ ⋯ $O_{COO-,AA}$) and also by the NH_2 moiety of AA and the carboxylic group of SPX (N-$H_{NH2,AA}$ ⋯ O-$H_{COOH,SPX}$). In the overall packing, the zig-zag chains of SPX alternate with AA, without any hydrogen bond being established between AAs (*Figure 9*).

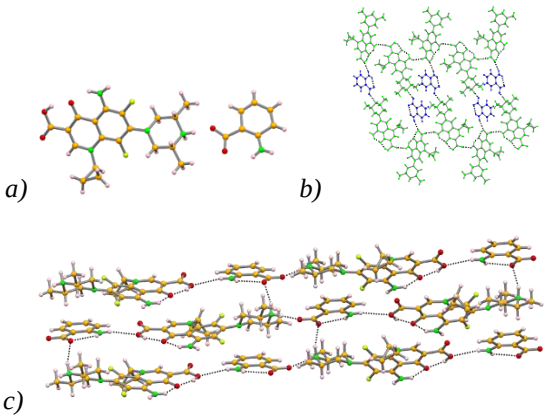

Figure 9 The illustration of SPX:AA crystal structure depicting a) the asymmetric unit; b) the hydrogen bonding between SPX and AA (blue); c) the crystal packing showing the alternance between SPX and AA

Furthermore, FT-IR and TGA-DSC measurements were also performed for all the forms obtained in this study. FT-IR results prove the formation of amine salts with the peaks at 1517 cm^{-1}, 1531 cm^{-1}, 1537 cm^{-1} ,1529 cm^{-1} as well as C=O asymmetric stretching at 1710 cm^{-1} for **SPX:4ASA Form II**, **SPX:3ABA Form I**, **SPX:3ABA Form II**, and **SPX:AA,** respectively (*Figure ES2, E3, ES4, ES5 (a)*). Asides from that, TGA-DSC results display the melting and decomposition starting at 203ºC, 252ºC, 250ºC, and 240ºC for **SPX:4ASA Form II**, **SPX:3ABA Form I**, **SPX:3ABA Form II**, and **SPX:AA,** respectively (*Figure ES2, ES3, ES4, and ES5 (b)*).

Solubility and stability tests

Solubility behaviour of all the forms obtained in this study were tested via an empirical method. All the multicomponent forms display enhanced solubility behaviour over SPX (*Figure 10*). Additionally, stability of all these forms were also investigated under 78% room humidity conditions, showing that all the forms are stable at least for 4 weeks (*Figure 11*)

Figure 10 Solubility behaviour of SPX, SPX:3ABA Form I, SPX:4ASA Form II, SPX:3ABA Form II, SPX:4ASA Form III, SPX:AA and SPX:4ASA Form I (from left to right)

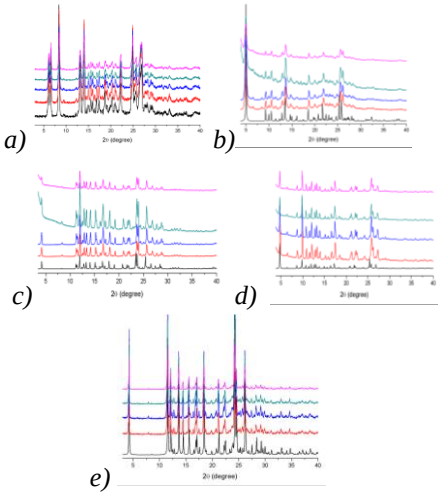

Figure 11 Stability behaviour of a) SPX:4ASA Form II b) SPX:4ASA Form III c) SPX:3ABA Form I d)SPX:3ABA Form II and e) SPX:AA under 78% humidity atmosphere for 4 weeks. Black, red, blue, green and pink lines are corresponding to simulated, 1st, 2nd ,3rd,4th week of experimental PXRD pattern respectively

Conclusion

To conclude, there are new crystalline forms of SPX with EtOH, and DMSO, whose crystal structure was not yet possible to obtain. An ACN solvate, induced by the presence of NA, has been characterizes even though a pure phase has never been obtained.

Regarding the co-crystal and multicomponent crystal forms screening, it is possible to conclude that there is proton transfer between SPX and 4-ASA, 3-ABA, AA, similar to theoretical expectations. These results highlight the relative strength of SPX as a base. For the synthesis of SPX and 4-ASA multicomponent salts, mechanochemistry has a superior activity over traditional solution chemistry method. It is worth mentioning that a superior antimicrobial activity is expected in the salts of SPX with 4-ASA since both compounds are antibiotics and they have shown to be effective in the treatment of tuberculosis through different pathways.

It is also noteworthy that all the new forms are stable and that they all are more soluble in water than SPX.

Experimental

All the reagents and solvents were purchased from Sigma-Aldrich, Fluka, Sigma, Aldrich and Alfa Aeser and used without further purification.

Synthetic procedures for the polymorphic screening of SPX

SPX-DMSO-S, Sparfloxacin in DMSO: 50 mg of SPX (0.127 mmol) was dissolved with 5 ml of DMSO at 120 °C and then, the solution was left to crystallize by slow evaporation of the solvent at RT.
*SPX-DMSO-Slu, Sparfloxacin in DMSO***:** 50 mg of SPX (0.127 mmol) was placed into a vial and subsequently 1 ml of DMSO solution was added. Afterwards, the solution was left stirring for 27 hours.
SPX-NA-S-ACN:EtOH, Sparfloxacin and Nalidixic acid in ACN:EtOH: The mixture of 0.06282 g of SPX (0.160 mmol) and 0.03717 g of NA (1:1 molar ratio) was dissolved in 6 ml of a 1:1 mixture of ACN:EtOH upon heating to 65ºC. The pH of the reaction medium was 5.5. At the end, the solution was left to crystallize by slow evaporation of the solvent at RT.

SPX-S-ACN:EtOH, Sparfloxacin in ACN:EtOH: 0.06282 g of SPX (0.160 mmol) was dissolved in 7 ml of solvent mixture of ACN:EtOH (1:1) upon heating to 65℃. Subsequently, the pH of the reaction medium was 6 and the solution was left crystallize by slow evaporation by the solvent at room temperature. Yet the solution did not yield any single crystals, and only crystalline powder was obtained.
SPX-NA-Slu-ACN:EtOH, Sparfloxacin and Nalidixic acid in ACN:EtOH: 0.06282 g of SPX (0.160 mmol) and 0.03717 g of NA (1:1 molar ratio) were stirred in 2 ml of a ACN:EtOH mixture at RT for 27 hours and left to evaporate.

The synthesis procedures of multicomponent forms of SPX

Synthesis of Sparfloxacin and 4- Aminosalicyclic acid salts

SPX:4ASA Form I: SPX (0.0357 g) and 4-ASA (0.0142 g), corresponding to 1:1 molar ratio, was dissolved with the addition of 20 ml (1:1) EtOH:H_2O solvent mixture at 50℃ for 10 minute. Later, the solution was left to crystallize by slow evaporation of the solvent at RT. Crystals with needle shape were obtained after 3-5 days, corresponding to **SPX:4ASA Form I**.

SPX:4ASA Form II: SPX (0.0539 g) and 4-ASA (0.0210 g), corresponding to 1:1 molar ratio, were placed into a mortar. Subsequently, the reagents were manually ground with the addition of 250 µl EtOH:H_2O (1:1) solvent mixture for 15 min. Light yellow powder was obtained, corresponding to SPX:4ASA Form II.
SPX:4ASA Form III: SPX (0.0626 g) and 4-ASA (0.0122 g), corresponding to 2:1 molar ratio, were placed into a mortar, subsequently, the reagents were manually grinded with the addition of 200 µl EtOH:H_2O (1:1) solvent mixture for 15 min. Light yellow powder was obtained, corresponding to SPX:4ASA Form III.

Synthesis of Sparfloxacin and 3- Aminobenzoic acid salts

SPX:3ABA Form I: SPX (0.0357 g) and 3-aminobenzoic acid (0.0124g), corresponding to 1:1 molar ratio, were placed into a flask and stirred for 27 hour with the addition of 1 ml of THF. Subsequently, the solution was left for drying at room temperature, corresponding to SPX:3ABA Form I.

SPX:3ABA Form II: SPX (0.0357 g) and 3-ABA (0.0124 g), corresponding to 1:1 molar ratio, was placed into a flask and stirred for 27 hour with the addition of 1 ml of H_2O. Afterwards, the solution was left for drying under room temperature, corresponding to SPX:3ABA Form II.

Synthesis of Sparfloxacin and Anthranilic acid salt

SPX:AA: SPX (0.0370 g) and anthranilic acid (0.0129 g), corresponding to 1:1 molar ratio, was dissolved with 8 ml of ACN:EtOH (1:1) solvent mixture at 80℃ for 30 minutes. Then, the solution was left to crystallize by slow evaporation of the solvent at RT. The formation of yellow needle crystals was observed within 3-5 days, corresponding to SPX:AA**.**

Characterization

Single crystal X-ray diffraction (SCXRD): Suitable single crystals of the acetonitrile solvate, SPX-4ASA Form I, II, III, and SPX:3ABA Form I, II as well as SPX:AA were selected and mounted on a loop with Fomblin protective oil. Data was collected on a Bruker AXS-KAPPA APEX II diffractometer and a Bruker AXS-KAPPA D8 – QUEST, at 293 K, with graphite-monochromated radiation (Mo K α, λ= 0.71073 Å). The X-ray generator was operated at 50 kV and 30 mA, and the APEX3 program monitored the X-ray data collection.

Table 1 Crystallographic details of SPX:4ASA Form I and II, SPX:AA, SPX:3ABA Form I and II, and SPX ACN solvate

Structure	SPX:4-ASA Form I	SPX:4-ASA Form II	SPX-AA
Empirical formula	C26 H36 F2 N5 O14	C13 H14 F N2.50 O3	C26 H28 F2 N5 O6
Formula weight	680.60 g/mol	272.77 g/mol	529.54 g/mol
Temperature	293(2) K	296(2) K	293 (2) K
Wavelength	0.71073 Å	0.71073 Å	0.71073 Å
Limiting indices	-17<=h<=17, -39<=k<=39, -8<=l<=8	-23<=h<=23, -8<=k<=8, -26<=l<=25	-23<=h<=23, -8<=k<=8, -26<=l<=25
Refinement method	Full-matrix least-squares on F^2	Full-matrix least-squares on F^2	Full-matrix least-squares on F^2
Crystal system	Monoclinic	Monoclinic	Orthorhombic
Space group	*P* $2_1/c$	*P* $2_1/n$	*Pbca*
Unit cell dimensions	a=14.2596(3)Å	a=18.5866(12)Å	a=7.5556(11)Å
	b=32.4372(5)Å	b=7.1168(5)Å	b=15.5026(2)Å
	c=7.1362(13)Å	c=21.1074(13)Å	c=41.4694(6)Å
	α = 90º	α = 90º	α = 90º
	β = 98.72(5)º	β = 94.127(3)º	β = 94.127(3)º
	γ = 90º	γ = 90º	γ = 90º

Volume	3262.4(10) Å^3	2784.8(3) Å^3	4856(13) Å^3
Z, calculated density	4, 1.386 mg/m^3	8, 1.301mg/m3	8, 1.449 mg/m^3
Reflections collected/unique	41239 / 6295 [R(int)=0.1413]	36119 / 5709 [R(int)=0.0674]	100518 / 5026 [R(int)=0.2272]
Data/ restraints/ parameters	6295 / 8 / 484	5709 / 6 / 378	5026 / 4 / 359
Absorption coefficient	0.120 mm $^{-1}$	0.102 mm $^{-1}$	0.112 mm $^{-1}$
F (000)	1428	1144	2224
Crystal size	0.14 x 0.08 x 0.04 mm	0.18 x 0.10 x 0.04 mm	0.40 x 0.06 x 0.02 mm
Theta range	2.374 to 25.903º	1.410 to 26.535º	2.628 to 26.511º
Completeness	99.9%	99.5%	100.0 %
Final R indices [I>2sigma(I)]	R1 = 0.1248, wR2 = 0.3449	R1 = 0.0693, wR2 = 0.2088	R1 = 0.1328, wR2 = 0.2217
R indices (all data)	R1 = 0.2105, wR2 = 0.4133	R1 = 0.1225, wR2 = 0.2532	R1 = 0.2501, wR2 = 0.2673
Goodness-of-fit on F^2	1.362	1.003	1.110
Large diff. peak and hole	1.691 and -0.792 e Å^{-3}	0.595 and -0.306 e Å^{-3}	0.588 and -0.363 e Å^{-3}
Extinction coefficient	n/a	n/a	n/a

Forms	**SPX:3-ABA Form I**	**SPX:3-ABA Form II**	**SPX ACN solvate**
Empirical formula	$C_{34.67}H_{41.33}F_{2.67}N_{6.67}O_8$	$C_{52}H_{58}F_4N_{10}O_{12}$	$C_{20}H_{23.50}F_2N_{4.50}O_3$
Formula weight	730.07 g/mol	1091.08 g/mol	412.93 g/mol
Temperature	293 (2) K	296(2) K	293 (2) K
Wavelength	0.71073 Å	0.71073 Å	0.71073 Å
Limiting indices	-52<=h<52,	-9<=h<9,	-38<=h<38,
	-9<=k<9,	-13<=k<13,	-11<=k<11,
	-19<=l<19	-20<=l<20	-17<=l<17
Refinement method	Full-matrix least-square on F^2	Full-matrix least-square on F^2	Full-matrix least-squares on F2
Crystal system, Space group	Orthorhombic *Pbca*	Triclinic *P-1*	Orthorhombic, Pcca
Unit cell dimensions	a=42.168 (5) Å	a=7.869(10) Å	a = 30.86 (4) Å
	b=7.757(10) Å	b=10.682(13)Å	b= 9.407(13)Å,
	c=15,618(19)Å	c=16,372(2) Å	c = 13.90(2) Å,
	α = 90º	α = 90º	α = 90º
	β = 90º	β = 90º	β = 90º
	γ=90º	γ=90º	γ = 90º
Volume	5109.0(11)Å^3	1341.0(3) Å^3	4038.9 Å^3
Z, calculated density	6.1424 mg/m^3	1.1351 mg/m^3	8.1358 mg/m ^{3}
Reflections collected/unique	32024/ 5211 [R(int)=0.0924]	13493 / 5368 [R(int=0.0596)]	99735/4125 [R(int)=0.165]
Data/ restraints parameters	5211 / 0 / 386	5368 / 6 / 386	4125 /3 /288
Absorption coefficient	0.112 mm $^{-1}$	0.106mm^{-1}	0.106 mm^{-1}
F (000)	2304	572	173
Crystal size	0.200 x 0.060 x 0.040 mm	0.200 x 0.800 x 0.050 mm	0.008 x 0.004 x 0.002 mm
Theta range	2.608-26.380º	2.915-26.420º	2.639-26.444º
Completeness	99.8 %	98.0 %	99.3%
Goodness-of-fit on F^2	1.099	1.014	1.146
Large diff. peak and hole	0.190 and -0.231e Å^{-3}	0.563 and -0.194 e Å^{-3}	0.390 e Å-3

Powder x-ray diffraction (PXRD): Samples were analysed by X-ray powder diffraction, using two diffractometers:

1- D8 Advance Bruker AXS θ-2θ diffractometer, with a copper radiation source (Cu Kα, λ= 1.5406 Å) and a SSD160 detector, operating at 40 kV and 30 mA. Throughout the measurements, Ni filter was used in the data collections

2- D8 Advance Bruker diffractometer, with a copper radiation source (Cu Kα, λ= 1.5406 Å) and a Linxeye-XE detector, operating at 40 kV and 30 mA. Throughout the measurements, no Ni filter was used in the data collections, relying in the capability of the detector to minimize Kβ.

Fourier Transform Infrared Spectroscopy (FT-IR): FT-IR analysis was performed by using Nexus-Thermo Nicolet spectrometer (64 scans and resolution of 4 cm−1) in the 4000−400 cm−1 range. Samples were prepared in KBr (1:100 in weight).

Differential Scanning Calorimetry (DSC) and Thermogravimetric Analysis (TGA): Both DSC and TGA was performed by using SETARAM TG-DTA 92 thermobalance under nitrogen flow with a heating rate of 10°C.min^{-1} for the sample (5-10 mg).

Preliminary/Empirical Solubility Studies: 10 mg of each new multicomponent form were added to 10 ml of H2O and stirred; as control, 10 mg of SPX were also added to 10 ml of water and stirred. The comparison between the clarity of the final solutions was used to estimate the relative solubility behaviour.

Stability tests: In order to investigate stability behaviour of all the forms obtained in this study, SPX:4ASA Form II and II, SPX:3ABA Form I and II as well as SPX:AA were placed into a desiccator with a saturated solution of NaCl (78% humidity) at room temperature. Afterward, PXRD measurements were performed every week for 4 weeks for all the forms mentioned above.

Acknowledgements

Authors acknowledge Fundação para a Ciência e a Tecnologia (FCT, Portugal), FEDER and Lisboa2020 for funding (projects UID/QUI/00100/2019, and PTDC/QUI-OUT/30988/2017. Dr Auguste Fernandes is acknowledged for the TGA and DSC data.

Notes and References

Electronic Supplementary Information (ESI) available: All the TGA, DSC and FTIR data obtained

are presented as supporting information. Relevant bond lengths and angles are also given.
Crystallographic information files (CIF) are accessible for all the crystal structures; they have also been deposited at the Cambridge Crystallographic Data Centre (CCDC).

1. Nangia, A. K.; Desiraju, G. R., Crystal Engineering: An Outlook for the Future. *Angewandte Chemie International Edition* **2019,** *58* (13), 4100-4107.
2. Moulton, B.; Zaworotko, M. J., From molecules to crystal engineering: supramolecular isomerism and polymorphism in network solids. *Chemical Reviews* **2001,** *101* (6), 1629-1658.
3. Kavanagh, O. N.; Croker, D. M.; Walker, G. M.; Zaworotko, M. J., Pharmaceutical cocrystals: from serendipity to design to application. *Drug discovery today* **2018**.
4. Aakeröy, C. B.; Fasulo, M. E.; Desper, J., Cocrystal or salt: does it really matter? *Molecular Pharmaceutics* **2007,** *4* (3), 317-322.
5. Shan, N.; Zaworotko, M. J., The role of cocrystals in pharmaceutical science. *Drug discovery today* **2008,** *13* (9-10), 440-446.
6. Fabbiani, F. P.; Allan, D. R.; Parsons, S.; Pulham, C. R., An exploration of the polymorphism of piracetam using high pressure. **2005**.
7. Khankari, R. K.; Grant, D. J., Pharmaceutical hydrates. *Thermochimica acta* **1995,** *248*, 61-79.
8. Rodriguez, C.; Bugay, D. E., Characterization of pharmaceutical solvates by combined thermogravimetric and infrared analysis. *Journal of pharmaceutical sciences* **1997,** *86* (2), 263-266.
9. Vishweshwar, P.; McMahon, J. A.; Bis, J. A.; Zaworotko, M. J., Pharmaceutical co-crystals. *Journal of pharmaceutical sciences* **2006,** *95* (3), 499-516.
10. Aakeröy, C. B.; Panikkattu, S.; DeHaven, B.; Desper, J., Interdependence of structure and physical properties in co-crystals of azopyridines. *CrystEngComm* **2013,** *15* (3), 463-470.
11. Kumar, S., Pharmaceutical Cocrystals: An Overview. *Indian Journal of Pharmaceutical Sciences* **2018,** *79* (6), 858-871.
12. Bolla, G.; Nangia, A., Pharmaceutical cocrystals: walking the talk. *Chemical Communications* **2016,** *52* (54), 8342-8360.
13. Thakuria, R.; Delori, A.; Jones, W.; Lipert, M. P.; Roy, L.; Rodríguez-Hornedo, N., Pharmaceutical cocrystals and poorly soluble drugs. *International journal of pharmaceutics* **2013,** *453* (1), 101-125.
14. Singh, S. S.; Thakur, T. S., New crystalline salt forms of levofloxacin: conformational analysis and attempts towards the crystal structure prediction of the anhydrous form. *CrystEngComm* **2014,** *16* (20), 4215-4230.
15. Martin, S. J.; Meyer, J. M.; Chuck, S. K.; Jung, R.; Messick, C. R.; Pendland, S. L., Levofloxacin and sparfloxacin: new quinolone antibiotics. *Annals of Pharmacotherapy* **1998,** *32* (3), 320-336.
16. Andersson, M. I.; MacGowan, A. P., Development of the quinolones. *Journal of Antimicrobial Chemotherapy* **2003,** *51* (suppl_1), 1-11.
17. Suh, B.; Lorber, B., Quinolones. *Medical Clinics of North America* **1995,** *79* (4), 869-894.
18. Wolfson, J. S.; Hooper, D. C., The fluoroquinolones: structures, mechanisms of action and resistance, and spectra of activity in vitro. *Antimicrobial agents and Chemotherapy* **1985,** *28* (4), 581.
19. Miyamoto, T.; Matsumoto, J.-i.; Chiba, K.; Egawa, H.; Shibamori, K.; Minamida, A.; Nishimura, Y.; Okada, H.; Kataoka, M.; Fujita, M., Synthesis and structure-activity relationships of 5-substituted 6, 8-difluoroquinolones, including sparfloxacin, a new quinolone antibacterial agent with improved potency. *Journal of medicinal chemistry* **1990,** *33* (6), 1645-1656.
20. Nakamura, S.; Minami, A.; Nakata, K.; Kurobe, N.; Kouno, K.; Sakaguchi, Y.; Kashimoto, S.; Yoshida, H.; Kojima, T.; Ohue, T., In vitro and in vivo antibacterial activities of AT-4140, a new broad-spectrum quinolone. *Antimicrobial agents and chemotherapy* **1989,** *33* (8), 1167-1173.
21. Pierfitte, C.; Royer, R. J.; Moore, N.; Bégaud, B., The link between sunshine and phototoxicity of sparfloxacin. *British journal of clinical pharmacology* **2000,** *49* (6), 609-612.

22. Gibbs, N. K., Drug-induced skin phototoxicity: lessons from the fluoroquinolones. In *Comprehensive Series in Photosciences*, Elsevier: 2001; Vol. 3, pp 337-356.
23. Outterson, K.; Powers, J. H.; Seoane-Vazquez, E.; Rodriguez-Monguio, R.; Kesselheim, A. S., Approval and withdrawal of new antibiotics and other antiinfectives in the US, 1980–2009. *The Journal of Law, Medicine & Ethics* **2013,** *41* (3), 688-696.
24. Gunnam, A.; Suresh, K.; Ganduri, R.; Nangia, A., Crystal engineering of a zwitterionic drug to neutral cocrystals: a general solution for floxacins. *Chemical Communications* **2016,** *52* (85), 12610-12613.
25. *Cambridge Structural Database* https://www.ccdc.cam.ac.uk/ (accessed June 15).
26. Llinàs, A.; Burley, J. C.; Prior, T. J.; Glen, R. C.; Goodman, J. M., Concomitant hydrate polymorphism in the precipitation of sparfloxacin from aqueous solution. *Crystal Growth and Design* **2008,** *8* (1), 114-118.
27. Shingnapurkar, D.; Butcher, R.; Afrasiabi, Z.; Sinn, E.; Ahmed, F.; Sarkar, F.; Padhye, S., Neutral dimeric copper–sparfloxacin conjugate having butterfly motif with antiproliferative effects against hormone independent BT20 breast cancer cell line. *Inorganic Chemistry Communications* **2007,** *10* (4), 459-462.
28. Vasiliev, A.; Golovnev, N., Crystal structure of two ionic sparfloxacin compounds. *Journal of Structural Chemistry* **2015,** *56* (5), 907-911.
29. Reddy, J. S.; Ganesh, S. V.; Nagalapalli, R.; Dandela, R.; Solomon, K. A.; Kumar, K. A.; Goud, N. R.; Nangia, A., Fluoroquinolone salts with carboxylic acids. *Journal of pharmaceutical sciences* **2011,** *100* (8), 3160-3176.
30. Huang, X.-F.; Zhang, Z.-H.; Zhang, Q.-Q.; Wang, L.-Z.; He, M.-Y.; Chen, Q.; Song, G.-Q.; Wei, L.; Wang, F.; Du, M., Norfloxacin salts with benzenedicarboxylic acids: charge-assisted hydrogen-bonding recognition and solubility regulation. *CrystEngComm* **2013,** *15* (30), 6090-6100.
31. Lubasch, A.; Erbes, R.; Mauch, H.; Lode, H., Sparfloxacin in the treatment of drug resistant tuberculosis or intolerance of first line therapy. *European Respiratory Journal* **2001,** *17* (4), 641-646.
32. Saifullah, B.; Hussein, M. Z.; Hussein-Al-Ali, S. H.; Arulselvan, P.; Fakurazi, S., Sustained release formulation of an anti-tuberculosis drug based on para-amino salicylic acid-zinc layered hydroxide nanocomposite. *Chemistry Central Journal* **2013,** *7* (1), 72.